Seismic Stability of a Multi-Storey Glulam Building Designed using Indonesian Timber Standards

Jerry Nansen[1] and Usman Wijaya[2*]
[1]Department of Civil Engineering
Universitas Kristen Krida Wacana
West Jakarta, 11470, Indonesia

[2]Department of Civil Engineering
Universitas Trisakti
West Jakarta, 11450, Indonesia
**usman.wijaya@trisakti.ac.id*

Date received: September 11, 2024
Revision accepted: July 9, 2026

Abstract

This study assesses the stability of a three-story glue-laminated timber (glulam) office building in Jakarta (Site Class SE, SDC D). Four alternative beam–column cross-sections (P1: 20×40; 20×20 cm, P2: 25×45; 25×25 cm, P3: 30×50; 30×30 cm, and P4: 40×60; 40×40 cm) were evaluated according to SNI 7973:2013, while the seismic parameters were determined according to SNI 1726:2019. Seismic response was assessed using the equivalent lateral force (ELF) procedure and linear time-history analysis (LTHA) with seven recorded ground motions scaled to the Jakarta MCEr target spectrum, assuming a semi-rigid diaphragm. Both procedures used a linear-elastic structural model, and the calculated displacements were amplified using the code-prescribed deflection amplification factor. The peak interstory drift ratio remained below 2% in both principal directions, with drift profiles consistent with first mode-dominated response. Models P2 and P3 met the strength and stiffness requirements while maintaining moderate drift, therefore providing the best balance under the assumptions adopted in this study. Section sizes within the P2–P3 range are recommended for this prototype, subject to adequate connection design. Further studies should examine taller or irregular buildings using explicit torsional checks and nonlinear connection models where inelastic behavior is of interest.

***Keywords**:* glue-laminated timber, seismic, stability, drift ratio

---

1. Introduction

Construction is one of the main causes of global warming. Carbon emissions generated during construction are a significant contributor to global warming. The use of materials with a high carbon footprint, such as cement, steel, and aluminum, should be avoided. The construction sector produced over 39% of the world's carbon emissions (Oosterveer, 2021). Therefore, reducing carbon emissions requires using sustainable materials, such as bamboo or wood, which can significantly lower the carbon footprint. For example, producing one ton of cement generates approximately 600 kg of CO_2 (Fennell *et al*., 2022). Sustainable design aims to minimize construction waste, use recyclable materials, and maximize the durability of structural designs (Iyengar, 2015).

Indonesia is one of the countries with the highest frequency of earthquakes in the world, ranging from mild to severe. One of the most significant earthquakes ever to occur in Indonesia struck Aceh in 2004. The magnitude 9.0 earthquake claimed approximately 283,000 lives and left 63,977 families homeless. In addition to Aceh, a significant earthquake also occurred in Yogyakarta in 2006, with a magnitude of 5.9, resulting in 5,700 fatalities (Astutik, 2020). The high number of casualties and building damage during the earthquake motivated the need for research on the structural strength of buildings to withstand earthquakes. Studies on timber structures show they are only 25% as heavy as reinforced concrete structures (Suyanto, 2020). This indicates that glulam structures have potential for use in low-rise buildings, as they can effectively resist lateral loads. Recent studies have focused on evaluating the seismic resistance of buildings in which glulam timber is the primary structural element (Huber *et al.*, 2018).

This study evaluates how alternative glulam beam-column dimensions affect the strength, stiffness, drift, and base shear of a low-rise Indonesian building designed in accordance with SNI 7973:2013 and SNI 1726:2019. Although the structural robustness and seismic response of multi-story timber buildings have been discussed in the literature, limited attention has been given to the combined effects of member-size variations and to comparing the equivalent lateral force procedure with linear-elastic LTHA using the same structural model. To address this gap, four member-size alternatives were evaluated for a three-story glulam office building in Jakarta using the Load Lateral Factor Design method and computational analysis. The study provides a code-based assessment of the trade-off among member size, seismic demand, drift, base shear, and material use, while supporting the broader application of sustainable structural materials in Indonesia.

2. Methodology

The research methodology comprised: establishing performance objectives for the three-story office timber frame (1); determining seismic parameters in accordance with SNI 1726:2019, including the site class, target spectrum, R, Ω_0, and Cd (2); defining glulam material properties and four member-size alternatives using LRFD in accordance with SNI 7973:2013 (3); performing linear-elastic finite element analyses using the ELF and LTHA procedures to obtain internal forces, story drift, and base shear (4); and verifying member strength, stiffness, amplified drift (≤ 0.02hsx), and P–Δ stability (5). The P1–P4 alternatives were then compared to identify the safest and most materially efficient solution.

2.1 Building Layout

The initial step in this design process is to gather structural data for the building. The structure to be designed is intended for use as an office building. This office building is planned to have three floors, with a total height of 10 meters, and is located in Jakarta, Indonesia. The floor plan and elevation view of the building are referred to as Figures 1 and 2, respectively.

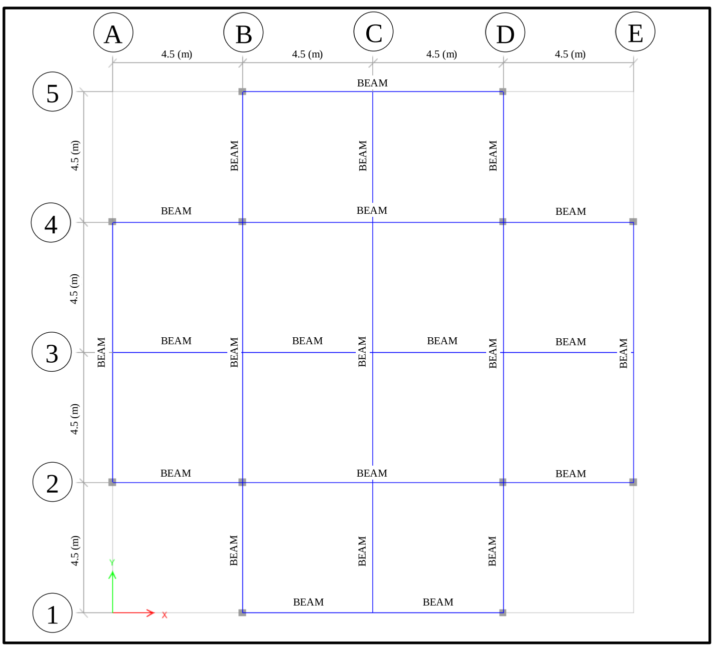

Figure 1. Floor plan

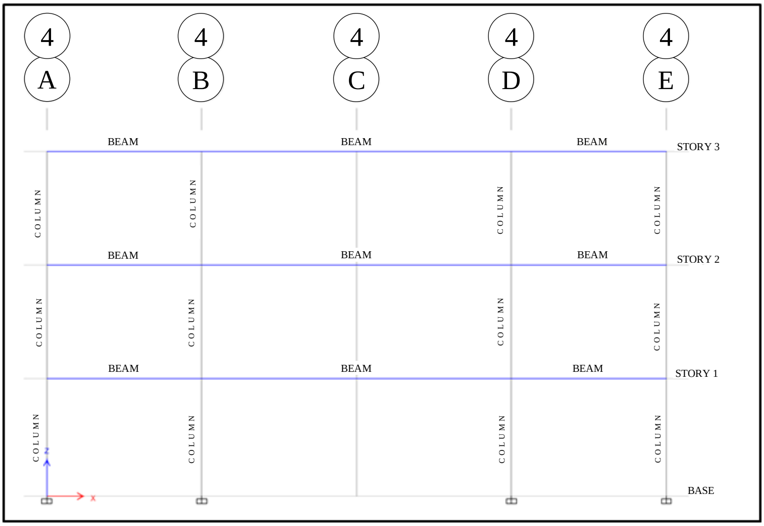

Figure 2. Elevation view

Based on the floor plan and section figures, alternative glulam beam–column dimensions were determined to align with the building layout. The initial dimensions were determined using the LRFD approach, referring to SNI 7973 to ensure compliance with strength and stiffness requirements. Four variants (P1–P4) in Table 1 were then evaluated to ensure the design's safety and feasibility. The dimensions used in this research can be analyzed using Load and Resistance Factor Design (LRFD) to estimate the strength of each column and beam. Each element of the structure must fulfill the required specifications to ensure the analysis results are considered safe. Furthermore, the floor slab is assigned as a semi-rigid diaphragm.

Table 1. Member classification

Model	Dimension (cm)	
	Beam	Column
P1	20×40	20×20
P2	25×45	25×25
P3	30×50	30×30
P4	40×60	40×40

In the P1 model, beams with dimensions of 20 cm × 40 cm and columns with dimensions of 20 cm × 20 cm were used. For the P2 model, beams with dimensions of 25 cm × 45 cm and columns with dimensions of 25 cm × 25 cm were implemented. In the P3 model, beams were 30 cm × 50 cm and columns were 30 cm × 30 cm. Lastly, for the P4 model, beams were 40 cm × 60 cm and columns were 40 cm × 40 cm.

2.2 Earthquake Parameter

As a basis for determining earthquake loads, seismic parameters are determined in accordance with SNI 1726:2019 for the case study location in Jakarta. The following Table 2 summarizes the risk categories and priority factors (I_e), mapped spectral accelerations (SS, S1), site classes (SE), along with coefficients F_a and F_v, and design spectral accelerations (SDS, SD1) resulting in Seismic Design Category D.

Table 2. Seismic parameter

Parameter	Value
Risk Category	I
Importance Factor (I_e) (*SNI 1726:2019*)	1.0
Mapped Spectral Response Acceleration	SS = 0.7806 S1 = 0.3823
Site Class	E
Site Class Coefficient	Fa = 1.276 Fv = 2.35
Seismic Design Category	D

While the values in Table 2 are used to construct the structural system and the design response spectrum, the base shear coefficient (C_s) is calculated, and the structure's drift and stability are evaluated in the following analysis stage, as shown in Table 3.

Table 3. Structural system

Structural system	*Glulam Frame*
Height (H)	10 m
Response Modification Coefficient (R)	1.5
Overstrength Factor (Ωo)	1.5
Deflection Amplification Factor (CD)	1.5
Periods,	
- Cu	1.4

- Ct	0.0488
- x	0.75
- Ta = Ct h_n^x	0.274 sec
- Cu Ta	0.384 sec
T_{model}	T_x = 1.75 sec T_y = 1.75 sec
T_{code}	0.384 sec
Cs = SDS / (R/Ie)	0.443
Cs_{max} = SD1 / (Tcode*(R/Ie))	1.040
Cs_{min} = 0.044*SDS*Ie	0.02921
Cs_{design}	0.443

Both the ELF and LTHA procedures used the same linear-elastic structural model. Seven recorded acceleration time histories were scaled to the Jakarta MCEr target spectrum and applied in the two principal directions. No nonlinear constitutive models, connection hysteresis, stiffness or strength degradation, or progressive failure mechanisms were included. Accordingly, the LTHA results represent record-specific linear dynamic responses and should not be interpreted as a direct simulation of inelastic structural behavior.

2.3 Load Resistance Factor Design

The load resistance factor design method is a structural design approach that ensures the adjusted strength of a structural element is not less than the capacity strength determined by the combination of LRFD load factors (Pranata & Suryoatmono, 2019). The load resistance factor design involves several key parameters, including load factors and correction factors. The correction factors to be considered in load resistance factor design include wet service factor (CM), puncture factor (Ci), temperature factor (Ct), format conversion factor (KF), time effect factor (λ), and resistance factor (ϕ).

To assess the structural strength in load resistance factor design, an analysis using the basic load resistance factor equation is necessary. The fundamental equation in load resistance factor design states that the adjusted strength must not exceed the structure's capacity strength. Based on the described factors, the basic equation is given by Equation 1.

$$R_u \leq \emptyset R_n \quad (1)$$

Where R_u is the ultimate strength capacity, R_n is the nominal strength.

2.4 Story Drift

Story drift refers to the difference in lateral displacement between two floors in a multi-story structure due to seismic effects (Hidayat & Loren, 2021). The story drift must be calculated as the ratio of the relative displacement between floors to the story height. This calculation is critical to ensure that the structure does not fail during an earthquake. The center of mass drift at level-x (δx) must be determined using Equation 2, and it must not exceed the allowable drift limit (Δa) of $0.020h_{sx}$ according to SNI 1726:2019.

$$\delta_x = \frac{C_d . \delta_{xe}}{I_e} \tag{2}$$

Where C_d is the lateral amplification factor, δ_x = required drift at level-x, I_e is the seismic importance factor, and h_{sx} is the height of the story at level-x.

2.5 Shear Force

According to SNI 1726:2019, the approximate fundamental period of vibration (T_a) is limited to prevent overly flexible structures (BSN, 2019). The fundamental natural period is crucial, as it significantly impacts the final results of the structural analysis, particularly in seismic design. Equation 3 is used to calculate the approximate period (T_a):

$$T_a = C_t . h_n^x \tag{3}$$

Where T_a is the period, C_t and x are empirical parameters depending on the type of structural system, and h_n is the height of the structure in meters.

The period value obtained from the calculation above is used to determine the value of ‘k’, which is used to calculate the seismic shear force distribution factor. The formula used to calculate the lateral seismic force acting on a specific floor is shown in Equations 4 and 5 (BSN, 2019):

$$CV_x = \frac{W_x \times H_x{}^k Floor}{W_x \times H_x{}^k Total} \tag{4}$$

$$F_x = V_x \times CV_x \tag{5}$$

Where W_x is the weight or mass of a specific floor, Hx is the height of the floor, Vx is the total base shear force, and $k = 1$ if $T \leq 0.5$ and $k = 2$ if $T \geq 2.5$.

2.6 Beam Design Analysis

According to the bending strength calculation using the load resistance factor design and SNI 7973:2013 standards, the structural design of beams involves several steps to ensure the beam meets safety requirements. The maximum moment obtained from computational software is a combination of 1.2 DL + 1.2 SDL + 1.6 LL + 0.5 LR. And with the time effect factor of 0.6, the factored bending moment could be obtained. The bending strength of the beam is calculated by using Equation 6 (BSN, 2013).

$$F^*_b = F_b \times \lambda \times \phi b \times KF \tag{6}$$

Where F^*_b is the factored bending strength; F_b = flexural strength value; λ is the time effect factor; ϕb is the resistance bending factor; KF = format conversion factor.

After calculating the bending strength of the beam, calculate the section modulus and corrected modulus of elasticity to find the corrected bending moment value. To obtain the section modulus, Equation 7 is used. In contrast, Equation 8 presents the corrected modulus of elasticity, and Equation 9 shows the corrected bending moment (BSN, 2013).

$$S_x = \frac{b \times d^2}{6} \tag{7}$$

$$E'_{min} = E_{min} \times \phi s \times KF \tag{8}$$

$$M' = F^*_b \times C_{fu} \times C_L \times S_x \tag{9}$$

Where S_x is the section modulus; b = width of beam; d = depth of beam; E_{min} is the minimum modulus of elasticity; ϕs is the resistance elasticity factor; KF = format conversion factor; C_{fu} is the flat use factor; C_L is the stability factor.

The calculation of shear strength using the Load Resistance Factor Design (LRFD) and SNI 7973:2013 standards utilized Equation 10 to determine the corrected shear strength and Equation 11 to calculate the shear capacity.

$$F^*_v = F_v \times \lambda \times \phi v \times KF \tag{10}$$

$$V' = F'_v \times \frac{2}{3} \times b \times d \quad (11)$$

Where F^*_v is the factored shear strength; F_v = flexural strength value; λ is the time effect factor; ϕb is the resistance bending factor; KF = format conversion factor.

To check the deflection of the beam under working loads, the maximum deflection was calculated using Equation 12, and the allowable deflection was calculated using Equation 13.

$$\triangle max = \frac{5}{384} \times \frac{(W_D+W_L)\times L^4}{E' \times I_x} \quad (12)$$

$$\triangle limit = \frac{L}{300} \quad (13)$$

Where W_D and W_L are the dead load and live loads; E' = adjusted modulus of elasticity; L is the span length of the beam; I_x is the moment of inertia; KF = format conversion factor.

2.7 Column Design Analysis

The dimensional analysis of the glulam columns used in this study complies with the requirements of SNI 7973:2013. The column dimensions are calculated for the structural design of office buildings. The initial step in column analysis involves checking both bending and axial strength. To calculate bending strength using the LRFD method, Equation 6 was utilized. The glulam material was assigned grade E10. The critical buckling value (F_{bE}) and bending stress (f_{b1}) are given by Equations 14 and 15. The essential buckling stress (F_{cE}) was calculated using Equation 16.

$$F_{bE} = \frac{1.2 \times E'_{min}}{Rb^2} \quad (14)$$

$$F_{b1} = \frac{Mu}{S_x} \quad (15)$$

$$F_{cE} = \frac{0.822 \times E'_{min}}{(\frac{l_e}{d})^2} \quad (16)$$

Where Rb is the slenderness ratio, E' = adjusted modulus of elasticity, Mu is the factored bending moment, and S_x is the section modulus.

The ratio must be ≤ 1.0. The ratio interactions 1 and 2 are represented in Equations 17 and 18. After verifying the column's compressive strength using the interaction ratios in Equations 17 and 18, the next step is to check the shear strength.

$$Ratio\ 1 = \left(\frac{f_c}{F'_c}\right)^2 + B_1 \times \frac{f_{b1}}{F'_{b1}} \tag{17}$$

$$Ratio\ 2 = \frac{f_c}{F_{cE2}} + \left(\frac{f_{b1}}{F_{bE}}\right)^2 \tag{18}$$

Where $B_1 = \frac{1}{1-\frac{f_c}{F_{cE1}}}$; F_{cE} is the critical buckling stress; F_{bE} is the critical buckling value; f_{b1} is the bending stress.

3. Results and Discussion

Seven ground-motion records were selected for Linear Time-History Analysis (LTHA) to represent three seismic-source mechanisms—shallow crustal thrust, Benioff-zone (intraslab subduction), and megathrust (interplate subduction)—in accordance with the response-history analysis provisions adopted in SNI 1726:2019. Three records represent shallow crustal events: the 1954 Northern California (Mw 6.50), 1976 Friuli, Italy (Mw 6.50), and 1983 Coalinga, California (Mw 6.36) earthquakes, which are moderate-magnitude shallow events with relatively high-frequency content. Two records represent Benioff-zone events: the 2011 Iwate, Japan (Hachinohe, Mw 7.40) and 2003 Tokachi-Oki, Japan (Chokubetsu, Mw 7.37) earthquakes, which reflect intermediate-depth subduction motions with longer durations than shallow crustal events. Two records represent megathrust events from the 2010 Chile earthquake (Mw 8.8; PEL and OLMU stations), providing long-duration, and large-magnitude motions. Together, the suite represents the principal seismic-source mechanisms relevant to the site and was scaled to the Jakarta MCEr target spectrum.

According to SNI 1726:2019, the story drift (Δi) must not exceed the allowable drift (Δa). For the glulam frame system, the deflection amplification factor is Cd = 1.5. Figure 3 compares the amplified drift-ratio profiles obtained from the ELF procedure and from LTHA using the seven ground-motion records scaled to the Jakarta MCEr target spectrum.

The drift-ratio profiles in Figure 3 increase toward the roof and are nearly coincident in the X and Y directions, consistent with the symmetric plan and the equivalent structural properties assigned in both principal directions. P1 produces the largest drift because it has the lowest lateral stiffness; P2 and P3 show intermediate responses; and P4 produces the smallest drift because the increase in stiffness outweighs the accompanying increase in seismic mass and base shear. For the selected and scaled records, the plotted LTHA drift demands are generally slightly lower than the ELF demands. This difference reflects the record-specific frequency content and dynamic response captured by LTHA; it is not evidence of inelastic behavior because both analyses use a linear-elastic model. The larger drift of P1 indicates greater flexibility, while its inadequacy is established separately by the beam and column checks in Tables 4 and 5. The analysis does not simulate yielding, connection degradation, or progressive structural failure. Conversely, the small drift of P4 indicates high lateral stiffness, but this benefit should be considered together with its higher material use, mass, and base shear.

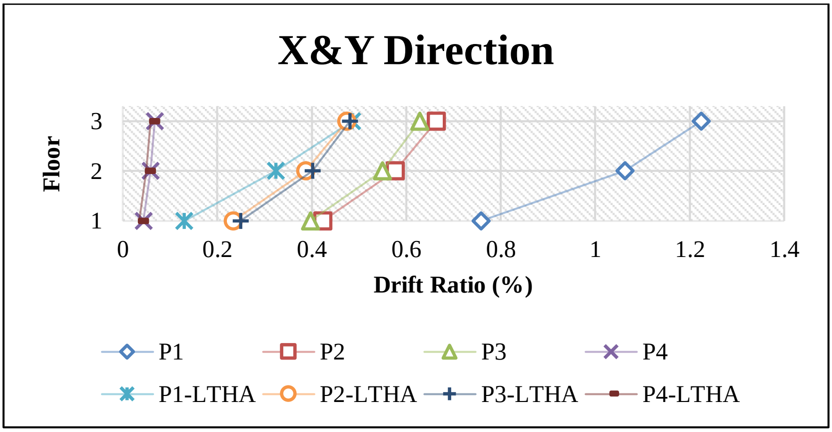

Figure 3. Story drift in the X and Y directions

Tao *et al*. (2024) investigated the seismic performance of a six-story timber moment-resisting frame with timber–steel hybrid beam-to-column joints. Although their study provides a relevant reference for multi-story timber structures, its drift results are not directly comparable to those of the present three-story glulam frame due to differences in building height, structural configuration, connection behavior, and analytical assumptions. In the present study, all peak inter-story drift ratios remained below the allowable limit of 2% specified in SNI 1726:2019. However, compliance with the drift limit alone does not demonstrate the absence of torsional irregularity, which requires an explicit comparison between the maximum edge drift and the average story drift, including accidental eccentricity effects. This code check remains necessary even for a nominally symmetric plan because accidental eccentricity represents uncertainties in mass location, stiffness distribution, and construction tolerances that are not captured by the idealized model. The restriction to a three-story, 10 m regular frame is also a limitation of this study. Higher-mode, P–Δ, and torsional effects may become more significant in taller or irregular buildings; therefore, the observed trends should not be extrapolated beyond the investigated prototype without additional analysis.

3.1 Base Shear

In the structural design of the building, the base shear induced by the seismic activities in both X and Y directions was obtained using finite element software. Following this, the inter-story shear forces were manually calculated using Equations 3 to 5. To determine the shear force at each floor, a linear static analysis was performed using the load values for each floor. Therefore, the inter-story shear is shown in Figure 4.

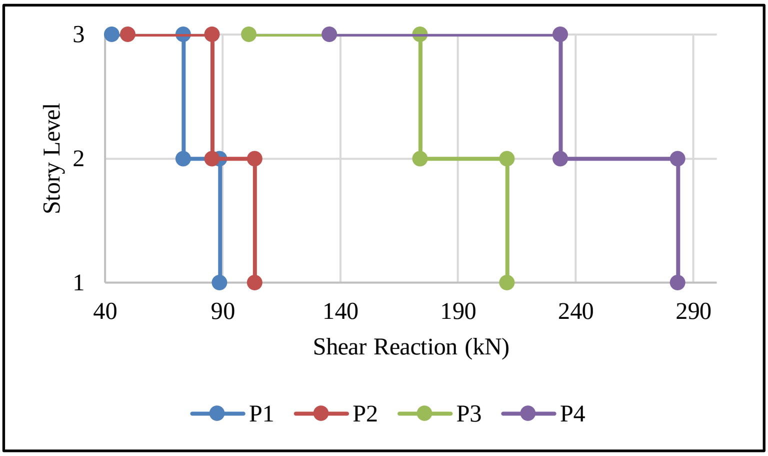

Figure 4. Story shear forces in the X and Y directions

The inter-story shear force curves in the X and Y directions overlap because the analyzed structure has a fully symmetric schematic plan. The building adopts identical bay spacing, story height, member dimensions, mass distribution, diaphragm constraints, and lateral-resisting system arrangement in both principal directions. As a result, the lateral stiffness, mass participation, and dynamic characteristics of the structure in the X and Y directions are essentially equivalent. Under the same seismic design parameters, this symmetry produces identical lateral responses, causing the inter-story shear force curves in both directions to coincide. Therefore, the overlapping curves do not indicate duplicated results, but rather reflect the symmetric behavior and equivalent lateral stiffness of the structural model in the two orthogonal directions. In addition, because the building is relatively low-rise and regular, the effect of higher-mode response and directional irregularity on the distribution of story shear is limited. The variation in shear force among the analyzed models is mainly governed by the structural mass and member dimensions. As the dimensions of structural components increase, the seismic weight and lateral force demands also increase, resulting in higher inter-story shear forces under seismic loading (Öberg *et al*., 2024).

3.2 Beam Design Results

Based on load resistance factor design calculations, the suitability of each beam dimension for models P1 through P4 is tabulated in Table 4.

Table 4. Beam design analysis

Beam Calculation	Model							
	P1		P2		P3		P4	
	Max	Limit	Max	Limit	Max	Limit	Max	Limit
Bending strength (kN.m)	71.11	69.31	74.70	109.81	77.32	162.75	81.91	312.72
Shear strength (kN)	9.80	68.42	10.80	96.37	11.88	128.35	14.30	205.33
Deflection (mm)	2.00	1.50	1.30	1.50	0.90	1.50	0.50	1.50

Based on this analysis, the beam dimensions for models P2 through P4 are adequate and meet the structural requirements. However, the dimensions used in model P1 do not meet the bending strength and beam stiffness criteria, indicating that the 20×40 cm beam dimensions are insufficient and do not comply with the necessary design standards.

3.3 Column Design Result

Based on the load-resistance factor design analysis, the suitability of each column dimension for models P1 through P4 is tabulated in Table 5.

Based on the analysis results, the modeling analysis using four different-dimension trials has largely met the requirements. The dimensional analysis of the elements across four different modeling trials shows that the dimensions of models P2 to P4 comply with the specifications. However, the use of dimensions for P1 does not meet the requirements due to non-compliance in the interaction 1 calculation of bending strength and axial compression. Thus, it can be concluded that the column with dimensions of 20×20 cm still does not meet the requirements. Model P1 was used as a reference to compare floor displacement and shear forces across different models.

Table 5. Column design analysis

Column Design		Model							
		P1		P2		P3		P4	
		Max	Limit	Max	Limit	Max	Limit	Max	Limit
Bending strength + axial compression	Ratio 1	2.82	1.00	0.97	1.00	0.90	1.00	0.39	1.00
	Ratio 2	0.11	1.00	0.03	1.00	0.03	1.00	0.11	1.00

4. Conclusion and Recommendation

For the investigated three-story (10 m) glulam frame in Jakarta (Site Class SE, SDC D), both the ELF procedure and LTHA, using seven ground-motion records scaled to the MCEr target spectrum, produced peak story-drift ratios below 2%, with profiles consistent with a first mode-dominated response. Because both analyses used a linear-elastic model, the results demonstrate compliance with the evaluated strength, stiffness, and amplified-drift criteria under the adopted assumptions; they do not directly quantify inelastic response, damage progression, or collapse capacity. The nearly identical X- and Y-direction drift and story-shear responses are consistent with the symmetric model, but they are not sufficient to establish the absence of torsional irregularity without the required edge-drift and accidental-eccentricity checks, which remain necessary even for nominally symmetric buildings. Of the four section alternatives, P1 (20×40; 20×20 cm) is inadequate because it fails the beam-bending/stiffness and column-interaction checks. P2 and P3 (25×45 cm and 25×25 cm, and 30×50 cm and 30×30 cm, respectively) provide the best balance among strength, stiffness, deformation, and material use for the investigated building. P4 (40×60; 40×40 cm) provides greater stiffness but also increases mass, base shear, and material use without a proportional performance benefit over P2–P3.

The study was intentionally limited to a three-story, 10 m regular prototype; therefore, the findings should not be generalized directly to taller buildings, where higher-mode, P–Δ, and torsional effects may be more significant. Accordingly, section sizes in the P2–P3 range are recommended for the investigated prototype, subject to project-specific verification of geometry, loading, material properties, and connection behavior. Connection design should be checked separately for strength, ductility, and cyclic performance, as these mechanisms were not explicitly modeled in the present linear analysis. Further studies should examine taller and irregular or asymmetric buildings, explicitly evaluate accidental torsion and P–Δ effects, and employ nonlinear material and connection models when assessing inelastic seismic performance.

5. Acknowledgement

The authors acknowledge the guidance and support received during this research.

6. References

Astutik, Y. (2020, September 28). Ini deretan gempa & tsunami besar di Indonesia. CNBC Indonesia. Retrieved September 10, 2024, from https://www.cnbcindonesia.com/news/20200928182916-4-190101/ini-deretan-gempa-tsunami-besar-di-indonesia

Badan Standardisasi Nasional. (2013). *SNI 7973:2013: Spesifikasi desain untuk konstruksi kayu*. Jakarta, Indonesia: Badan Standardisasi Nasional.

Badan Standardisasi Nasional. (2019). *SNI 1726:2019: Tata cara perencanaan ketahanan gempa untuk struktur bangunan gedung dan non gedung*. Jakarta, Indonesia: Badan Standardisasi Nasional.

Fennell, P., Driver, J., Bataille, C., & Davis, S.J. (2022). Going net zero for cement and steel. *Nature, 603,* 574–577. https://doi.org/10.1038/d41586-022-00758-4

Hidayat, I., & Loren, M. (2021). Comparison of seismic load calculation based on SNI 1726-2012 and SNI 1726-2019 to capacity of elements on low level building. In *Proceedings of the 4th International Conference on Eco Engineering Development* 2020, Banten, Indonesia, 012047. https://doi.org/10.1088/1755-1315/794/1/012047

Huber, J.A.J., Ekevad, M., Girhammar, U.A., & Berg, S. (2018). Structural robustness and timber buildings — A review. *Wood Material Science & Engineering, 14*(2), 107–128. https://doi.org/10.1080/17480272.2018.1446052

Iyengar, K. (2015). Sustainable architectural design: An overview. New York, United States: Routledge. https://doi.org/10.4324/9781315758473

Öberg, V., Jockwer, R., & Goto, Y. (2024). Design for structural adaptation in timber buildings: Industry perspectives and implementation roadmap for Sweden and Australia. *Journal of Building Engineering, 98,* 111413. https://doi.org/10.1016/j.jobe.2024.111413

Oosterveer, P. (2021). How the built environment must respond to the IPCC's 2021 climate change report. Arcadis. Retrieved from https://www.arcadis.com/en/insights/blog/global/peter-oosterveer/2021/how-the-built-environment-must-respond-to-the-ipccs-2021-climate-change-report

Pranata, Y.A., & Suryoatmono, B. (2019). Struktur kayu: Analisis dan desain dengan LRFD. Bandung, Indonesia: PT Remaja Rosdakarya.

Suyanto, I.R. (2020). Perilaku cross-laminated timber (CLT) sebagai material utama bangunan tingkat menengah tahan gempa di Indonesia. *Rekayasa Sipil, 14*(3), 204–210. https://doi.org/10.21776/ub.rekayasasipil.2020.014.03.6

Tao, H., Yang, H., Wu, Y., Ju, G., Liu, J., & Shi, B. (2024). Seismic performance of a six-story timber moment-resisting frame with timber-steel hybrid beam-to-column joints. *Structures, 71*, 108070. https://doi.org/10.1016/j.istruc.2024.108070